

Exploring the Timescale Limitations of RoboClam: A Biologically Inspired
Burrowing Robot

by

Monica Isava

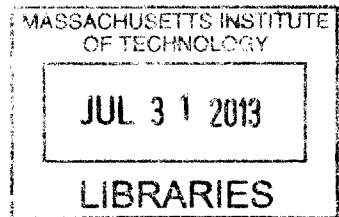
Submitted to the
Department of Mechanical Engineering
in Partial Fulfillment of the Requirements for the Degree of
Bachelor of Science in Mechanical Engineering

at the

Massachusetts Institute of Technology

June 2013

ARCHIVES



© 2013 Monica Isava. All rights reserved.

Signature of Author: _____
Department of Mechanical Engineering
May 10, 2013

Certified by: _____
Amos Winter
Assistant Professor of Mechanical Engineering
Thesis Supervisor

Accepted by: _____
Anette Hosoi
Professor of Mechanical Engineering
Undergraduate Officer

Exploring the Timescale Limitations of RoboClam: A Biologically Inspired Burrowing Robot

by

Monica Isava

Submitted to the Department of Mechanical Engineering
on May 10, 2013 in Partial Fulfillment of the
Requirements for the Degree of

Bachelor of Science in Mechanical Engineering

ABSTRACT

The Atlantic razor clam (*Ensis directus*) burrows into soil by contracting its valves in a pattern that fluidizes the particles around it. In this way, it uses an order of magnitude less energy to dig to its burrowing depth than would be expected if it were moving through static soil. This technology is a mechanically simple solution to reduce energy requirements in applications such as anchoring and underwater pipe installation. RoboClam is a robot that imitates the movements of *Ensis* and has achieved localized fluidization in environments similar to that of the animal.

This paper tests the theoretical timescale limits for running RoboClam while still achieving the soil fluidization that *Ensis* achieves. Needle valves were used on the robot's pneumatic control system to vary its expansion and contraction times in a series of tests, then each test was analyzed to determine to what extent soil fluidization occurred. It was found that the theoretical minimum contraction time is an appropriate boundary and the theoretical maximum contraction time is a loose boundary on tests that will result in soil fluidization. However, these conclusions came from a limited number of tests, so further testing is necessary to confirm these results.

Thesis Supervisor: Amos Winter
Title: Assistant Professor of Mechanical Engineering

Table of Contents

Abstract	2
Table of Contents	3
List of Figures	4
1. Introduction	5
1.1 Ensis Directus	5
1.2 RoboClam Design and Control	8
1.3 Previous RoboClam Tests	10
2. Preparing for Timescale Testing of RoboClam	14
2.1 Manipulating Expansion and Contraction Times Using Needle Valves	14
2.2 The Solenoid Valve Control System	15
2.3 Finding Optimal Desired In/Out Times	17
3. Timescale Testing of RoboClam and Results	20
3.1 Running Timescale Tests	20
3.2 Results from Timescale Tests	21
3.3 Observations from Test Results	22
4. Conclusions and Future Work	24
4.1 Conclusions	24
4.2 Automating Tests	25
4.3 Varying Pressures with Flow Rates	25
5. Bibliography	27

List of Figures

Figure 1-1:	A visualization of the burrowing cycle of <i>Ensis directus</i>	6
Figure 1-2:	Comparison of the energy expended by <i>Ensis</i> and the energy needed to push a blunt body of the same shape to burrow depth	7
Figure 1-3:	Design of RoboClam	9
Figure 1-4:	A schematic of the pneumatic control system for each of the motions in RoboClam	10
Figure 1-5:	Results of 362 past tests in varying the contraction and expansion times of RoboClam	11
Figure 2-1:	A schematic of the updated pneumatic control system for the in and out motions in RoboClam	15
Figure 2-2:	A graph of desired and actual in/out displacements for an end effector hanging in midair	17
Figure 2-3:	A graph of desired vs. actual in/out displacement for an end effector suspended in midair with the desired in/out times optimized	18
Figure 3-1:	An example of the robot's vertical displacement over time for a given trial	21
Figure 3-2:	Results of 53 tests in varying the contraction and expansion times of RoboClam using needle valves	22

1. Introduction

The aim of the research presented in this thesis is to understand the capabilities of a robotic imitation of a small underwater burrowing animal. This technology is relevant in a wide range of applications, including anchoring, underwater sensor placement, and subsea pipe installation. It is important to understand the functionality and limits of such a device in order to both optimize the process by which it digs and to pursue further applications, such as deepwater digging. This thesis focuses on finding the timescale limitations of the RoboClam, a robot that imitates the burrowing ability of *Ensis directus*, the Atlantic razor clam.

The remainder of this chapter will focus on the digging patterns of *Ensis*, the design and control system of the RoboClam, and the results of past timescale tests on the RoboClam [1]. The second chapter describes the experimental design and methodology of the new timescale tests, and the third chapter presents and discusses the results of these tests. The fourth chapter gives conclusions based upon the data collected, as well as considerations for future work with the RoboClam.

1.1 *Ensis Directus*

Ensis directus, the Atlantic razor clam, is composed of a long, thin body covered by a shell made of two valves that contract radially inward and outward. It also has a foot at the end of its body, which is a soft organ that can pull the whole body downward or

push it upward. The clam digs into soil using a series of up, down, in, and out motions as shown in Figure 1-1 [2].

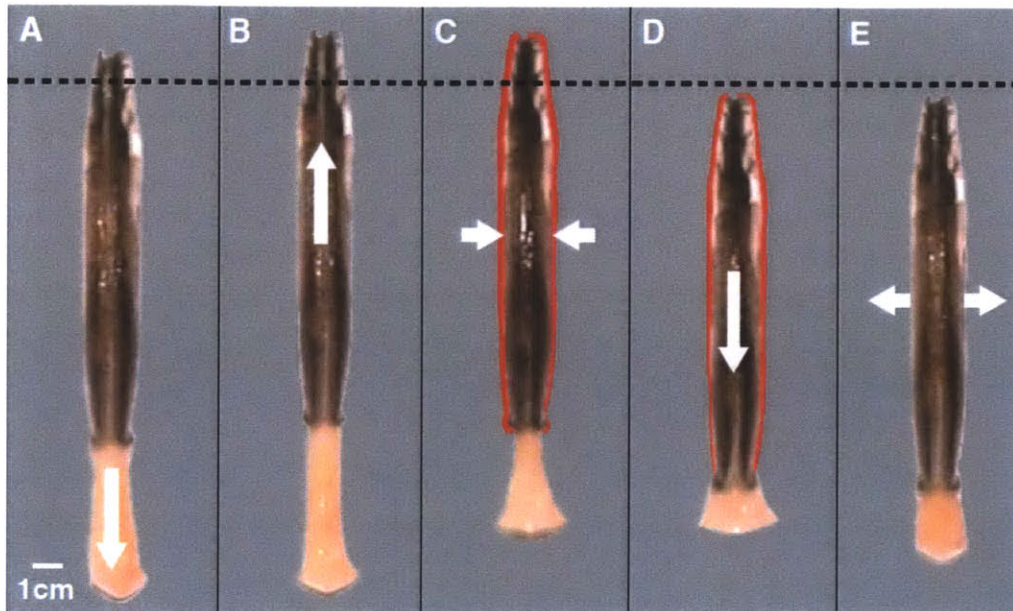


Figure 1-1: A visualization of the burrowing cycle of *Ensis directus*. The horizontal dotted line indicates a constant depth for reference, the white arrows indicate movements of the foot or valves, and the red area indicates the void that the clam leaves after contracting. A) Start of digging cycle. B) Foot extends, lifting body. C) Valves contract, leaving void space around animal and pushing blood to the foot so it can serve as an anchor. D) Foot retracts, pulling body downward through the void. E) Valves expand to begin next digging cycle.

The movements of *Ensis* are unique in that they cause the fluidization of the soil around the animal. Normally, in a Newtonian fluid, viscosity and density do not change with depth. However, in a granular solid (such as soil), the particles experience contact stresses, and thus frictional forces, that scale with surrounding pressure. Thus, they experience shear stresses that increase linearly with depth [3]. This means that inserting devices into sand can be energetically costly, since insertion forces $F(z)$ will increase linearly with depth z [4], so insertion energy $E = \int F(z) dz$ will scale with depth squared.

However, when *Ensis* moves its valves, the particles in the void around it fluidize (behave more like a Newtonian fluid) and thus the energy required to dig through them scales linearly with depth rather than with depth squared. Therefore, *Ensis* uses far less energy than expected to dig to burrow depth. This phenomenon was explored and confirmed in tests that compared the energy expended by *Ensis* to the energy required to push a blunt body of the same size into soil, both as functions of depth. The results of this study are shown in Figure 1-2 [1]. These results demonstrate that *Ensis* uses a full order of magnitude less energy to dig to its burrowing depth than would a blunt body. The ability of *Ensis* to dig using so much less energy than expected, combined with the simplicity of its burrowing movements, make it a desirable subject for biomimetics in burrowing.

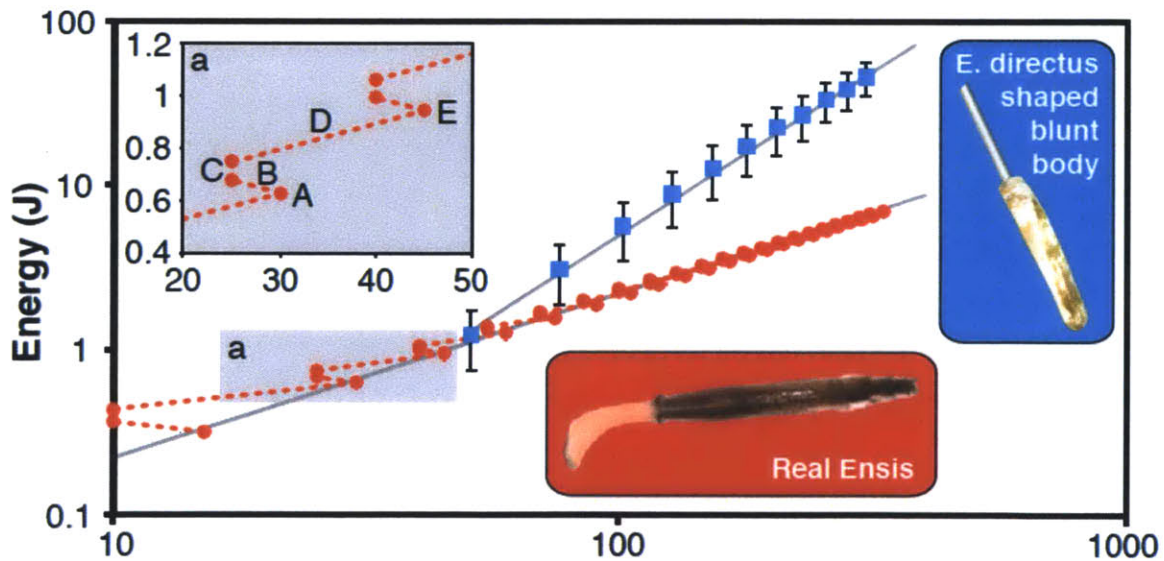


Figure 1-2: Comparison of the energy expended by *Ensis* and the energy needed to push a blunt body of the same shape to burrow depth. Because *Ensis* moves through locally fluidized soil, it requires an order of magnitude less energy to reach a given depth than would an *Ensis*-shaped blunt body being pushed into the soil.

1.2 RoboClam Design and Control

Because *Ensis* is so energetically efficient in its burrowing techniques, there are many potential applications for a mechanical system that could dig like it. The RoboClam was developed precisely to explore these possible applications. It was designed to imitate the motions of *Ensis directus* and thus dig into soil using an amount of energy that scales linearly with depth. The basic design of the RoboClam is shown in Figure 1-3. The end effector is the most fundamental piece, as it is the part that actually digs into soil by imitating the movements of *Ensis*. Its movements are controlled by two pistons, an upper piston and a lower piston. The upper piston is connected to a rod that is in turn connected to a wedge inside the end effector. As the wedge moves up and down, it slides along railings that make the end effector walls move in and out, thus imitating the in/out motions of the clam. The lower piston is connected to a larger rod that is in turn connected to the end effector itself. It moves the entire end effector up and down as it moves up and down, thus imitating the up/down motions of the clam.

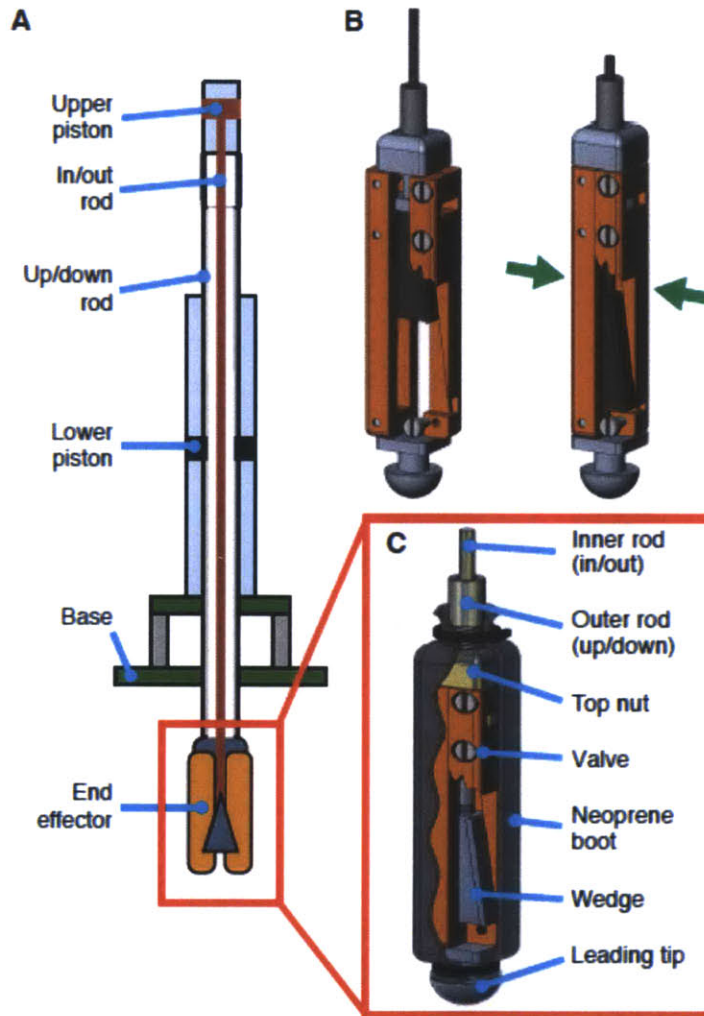


Figure 1-3: Design of RoboClam. A) Basic schematic of the robot design. The upper piston moves the end effector in and out, while the lower piston moves it up and down. B) Inward motion of the end effector as the wedge slides down its railings. C) Cutaway view of the entire end effector. The neoprene boot protects the end effector from soil particles that could jam it, the inner rod connects to the wedge to control the end effector's in/out motion, and the outer rod connects to the top nut to control the end effector's up/down motions. The leading tip imitates the round end of *Ensis* so that the end effector can enter the soil smoothly.

The motions of RoboClam are entirely controlled by a pneumatic system, which is depicted in Figure 1-4. This pneumatic system exists for each of the four motions (up, down, in, and out) necessary for the robot to dig. When a certain motion is desired, the solenoid valve corresponding to that motion switches on, letting pressurized air go

through it to move the corresponding piston in the desired direction. By sending a series of signals to the solenoid valves, we can move the pistons in such a way that the end effector imitates the movements of *Ensis*.

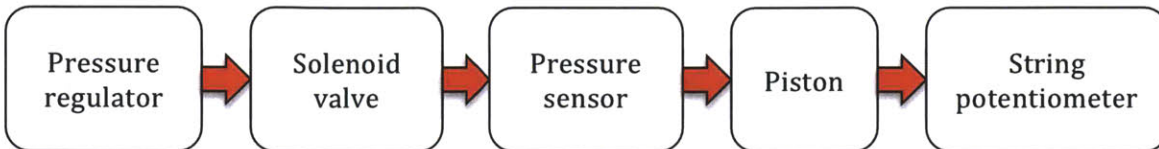


Figure 1-4: A schematic of the pneumatic control system for each of the motions (up, down, in, out) in RoboClam. The air goes through a pressure regulator, which sets it to a specified pressure. It then goes through a solenoid valve that acts as an on/off switch, which is on when the specified motion (up, down, in, or out) is needed. It then goes through a pressure sensor that measures the actual air pressure just before entering the chamber with the piston. It then moves the piston, which in turn moves the end effector either up, down, in, or out. The piston’s movements are tracked by a string potentiometer, which measures displacement.

1.3 Previous RoboClam Tests

One important consideration when finding the optimal way to run RoboClam is the speed at which the valves open and close. Since the clam’s low-energy digging relies on the fluidization of the particles around it, it can be imagined that there would be some speeds at which the valves would be either moving too quickly or too slowly to allow the soil around them to fluidize properly. This hypothesis was the basis of tests done on RoboClam by Amos Winter, Robin Deits, and Daniel Dorsch [1]. In these tests, RoboClam repeatedly dug into a 33-gallon drum full of 1mm diameter soda lime glass beads, saturated with tap water (to imitate the sand in *Ensis*’s natural habitat), with the end effector moving only in and out (corresponding to motions C and E in Fig. 1-1). The expansion and contraction times (t_{out} and t_{in} , respectively) were varied between tests by a

genetic algorithm (GA) [5], which generates a series of parameters (in our case, the pressures supplied to the in and out valves) and adjusts them to try to achieve the lowest “cost.” This “cost” was measured by the power law relationship, α , between the energy expended by the robot, E , and the depth of the tip of the end effector, δ , where $E = \kappa\delta^\alpha$ and $\ln\kappa$ is the vertical intercept on the power law plot. Values of α close to 1 were indicative of burrowing via local fluidization (where energy scales linearly with depth), and values of α close to 2 were indicative of burrowing in static soil (where energy scales with depth squared). There were a total of 362 tests run, and the results from these tests are shown in Figure 1-5.

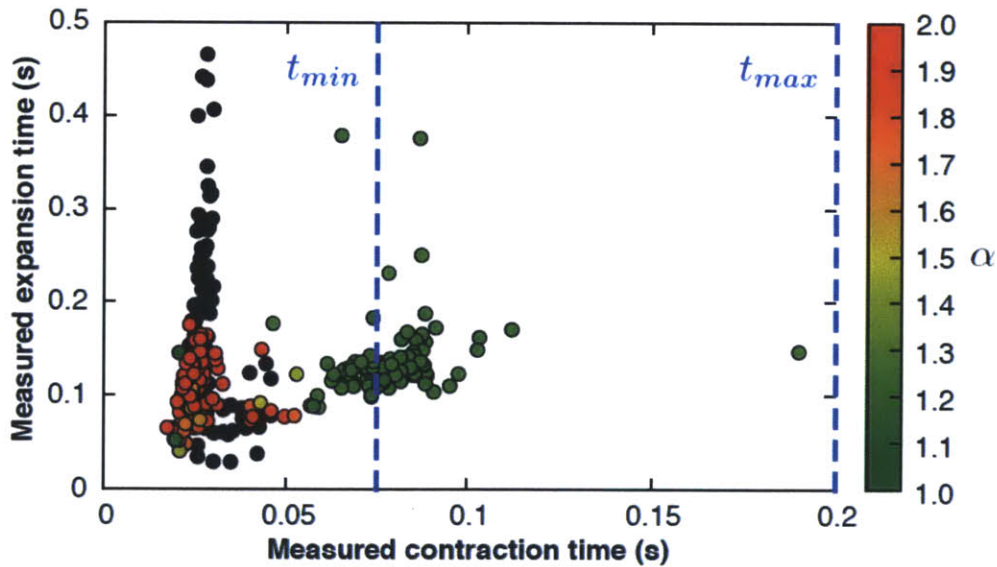


Figure 1-5: Results of 362 past tests in varying the contraction and expansion times of RoboClam. The color of the points correspond to the power law relationship α between energy and depth, where $E = \kappa\delta^\alpha$ and $\ln\kappa$ is the vertical intercept on the power law plot. Values of α close to 1 imply digging with localized fluidization, whereas values of α close to 2 imply digging in static soil. Black dots were tests that were deemed unsuccessful because the end effector failed to burrow further than one full body length. Timescales t_{min} and t_{max} correspond to the calculated minimum and maximum contraction times needed to achieve localized fluidization.

The calculated minimum and maximum contraction times shown in Fig. 1-5, t_{min} and t_{max} , come from the theory of soil fluidization. In order to calculate t_{min} , we use Stokes drag, which quantifies the advection time, or the amount of time necessary for the particles to speed up to the velocity of the valve contraction. We can imagine that if the valves contract too quickly, then the particles won't have enough time to fill the void left by the contraction, and thus the particles won't fluidize. The Stokes drag analysis yields a value of $t_{min} \approx 0.075s$, which is confirmed by the prevalence of green dots beginning at about that contraction time in Fig. 1-5 [1].

In order to calculate t_{max} , we examine the friction angle of the soil, which determines the point at which the particles will collapse and landslide around the end effector as it contracts, rather than fluidizing. Analyzing the effective stresses in the soil along with the friction angle yields a value of $t_{max} \approx 0.2s$, but the tests from Figure 1-5 did not reach this contraction time [1]. Testing this theoretical value of t_{max} was one of the main objectives of the research presented in this thesis.

There is also a theoretical maximum value for the expansion time, which results from the settling time of the particles, or the time required to move through the fluidized substrate and re-expand before it settles. An analysis of the settling time yields a value of $t \approx 2.0s$, a value well above the maximum expansion time in the tests above [1]. Because this value is so far from the expansion times of the given tests, it was concluded that expansion time wouldn't have a significant effect on whether or not the robot achieved soil fluidization, and thus experiments were not designed specifically to test the validity of this maximum time.

The results of the tests above validated the existence of the theoretical minimum contraction time, but they were too closely concentrated around low values of $t_{contract}$ and t_{expand} to provide conclusions about higher timescales. Therefore, the purpose of the research for this thesis was to run tests across a wider sampling of t_{expand} and $t_{contract}$ in order to assess the range of timescales in which RoboClam could achieve localized fluidization.

2. Preparing for Timescale Testing of RoboClam

In order to run the desired timescale testing on RoboClam, needle valves were added to the pneumatic control systems for the in and out valves. Optimal testing parameters for the solenoid valves were then determined for each chosen pair of needle valve settings.

2.1 Manipulating Expansion and Contraction Times Using Needle Valves

Since the genetic algorithm (GA) used in previous tests, which mainly changed the pressures of the air sent to the in and out valves, was not able to significantly slow down the expansion and contraction movements of the robot, it was determined that needle valves would be used instead to test the efficacy of slower expansion and contraction times. Needle valves were inserted just before the pressure sensors in the pneumatic control systems for the in and out valves, as shown in Figure 2-1. With this setup, partially opening and closing the needle valves would change the flow rate of the air into the area above or below the piston, therefore changing the time it took to fully expand or contract the end effector.

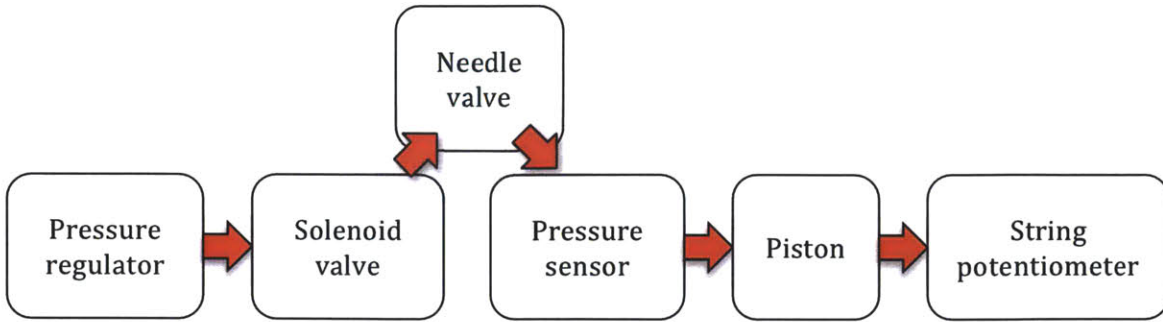


Figure 2-1: A schematic of the updated pneumatic control system for the in and out motions in RoboClam. The needle valve was added between the solenoid valve and the pressure sensor to regulate the flow rate of air into the area above or below the piston such that t_{expand} and $t_{contract}$ could be manually varied.

One kind of needle valve was used for the in valve, and another was used for the out valve, in order to accommodate for the differences in desired variability in testing. Since it was more important to vary $t_{contract}$ in order to validate the theoretical maximum contraction time, than to vary t_{expand} , a large valve with high variability of flow coefficients was chosen for the contracting valve. Contrastingly, since it was not as important to vary t_{expand} , a medium-sized valve with less flow coefficient variability was chosen for the expanding valve. The final chosen valves were a Swagelok SS-4L valve for the contracting valve and a Swagelok SS-1RM4 valve for the expanding valve. For each of these valves, five settings (quantified by number of turns closed) were chosen for testing. These settings served as a representative sample of air flow rates available for each needle valve.

2.2 The Solenoid Valve Control System

Before determining the optimal testing parameters for the needle valves, it is important to understand the solenoid valve control system. The solenoid valves open and

close to allow and restrict airflow to the needle valves, and they do this by responding to the best of their ability to desired time and displacement parameters sent to them.

The in/out solenoid valves take four inputs: in time, out time, in displacement, and out displacement. They then create a desired movement graph, as shown by the red line in Figure 2-2, and match that graph to the best of their ability. A lower (more negative) displacement corresponds to a more closed end effector, and a higher (less negative) displacement corresponds to a more open end effector. Therefore, if the desired displacement is higher than the current displacement, the “out” solenoid valve will open. Similarly, if the desired displacement is lower than the current displacement, the “in” solenoid valve will open. Since the desired (red) graph exceeds the physical opening and closing limits of the end effector, the solenoid valves will open repeatedly for the duration of $t_{out_desired}$ or $t_{in_desired}$, even when the end effector has reached its maximum in or out position. This continual reopening of the solenoid valves to try to reach an unattainable position can be seen in the jagged parts of the blue line in Figure 2-2, in which each spike corresponds to a solenoid valve reopening to try to push its corresponding piston farther than it can go. The problem here lies not in the desired displacements but in the desired times. Adjusting the desired times to match the actual opening/closing times will cause each solenoid valve to only open once, followed by the opposite valve opening. This desired time optimization is the focus of Section 2.3.

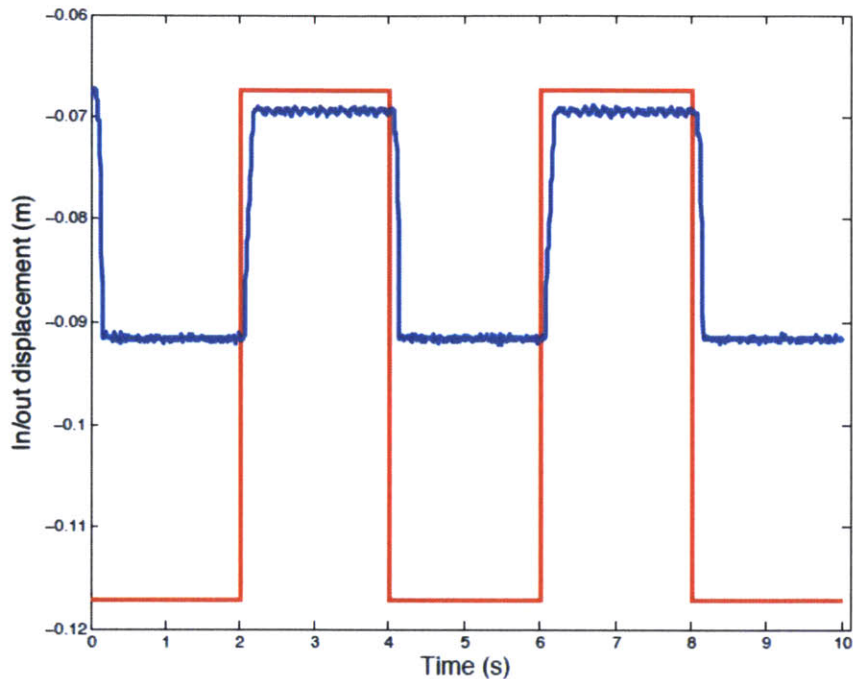


Figure 2-2: A graph of desired and actual in/out displacements for an end effector hanging in midair. The desired pattern (determined by the desired in/out times and desired in/out displacements) is shown in red, and the measured displacement is denoted in blue. Any time the desired displacement is lower than the measured displacement, the “in” solenoid valve opens, and any time the desired displacement is higher than the measured displacement, the “out” solenoid valve opens. The jagged blue lines correspond to times when the end effector has already reached its maximum expansion or contraction, but the solenoid valves continue to reopen in order to try to reach the desired displacement.

2.3 Finding Optimal Desired In/Out Times

For each combination of needle valve settings (i.e. a setting for the “in” valve and a setting for the “out” valve), it was necessary to determine the optimal desired parameters before running tests. As was briefly discussed in Section 2.2, the desired in and out displacements were determined to be unimportant, so long as they encompassed the full range of in/out motion of the end effector. If they satisfied this condition, they

would allow the end effector to expand and contract completely. Therefore, this section will focus instead on finding the optimal desired in/out times.

Finding the optimal desired in/out times was an iterative process. For each pair of needle valve settings, the end effector was suspended in midair and the desired in and out times were adjusted until they were long enough that the end effector could expand/contract as far as possible, but short enough that the solenoid valves didn't reopen after reaching their maximum displacement, as was seen in Figure 2-2. An example of an in/out displacement graph with optimized desired times is shown in Figure 2-3.

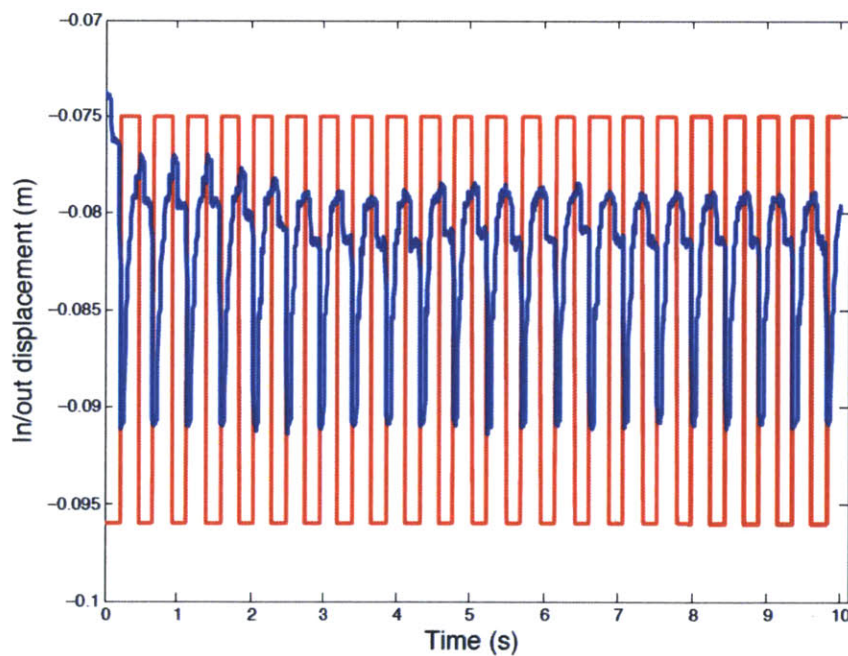


Figure 2-3: A graph of desired vs. actual in/out displacement for an end effector suspended in midair with the desired in/out times optimized. The desired displacements are in red and the measured displacements are in blue. If the desired times were any longer, the solenoid valves would open several times at the bottom or top of the cycles, and if they were any shorter, the end effector wouldn't have enough time to reach its maximum expanded or contracted position.

Note that the optimal desired in/out times were determined with the end effector hanging in thin air, whereas the actual tests would be run with the end effector digging through a sand-like substrate. To confirm that the surrounding substrate didn't modify the optimal desired times, the optimal time settings were also found while the end effector dug into the substrate for a few needle valve settings. These optimal time settings were found by the same process as above, and through these tests, it was determined that the optimal desired in/out times were the same regardless of whether the end effector was in midair or digging into sand.

Another thing to note is that as the needle valves got closer to closing and air flow got more restricted, the amplitude of the in/out motions got smaller, meaning that the end effector didn't reach its completely open or completely closed state. This problem could be related to the air pressure given by the pressure regulator (which was not varied during these tests). It is possible that for low flow rates, higher pressures are needed to allow the end effector to still reach its maximum amplitude, but this possibility was not explored in detail during the research for this thesis. It is, however, a possibility that should be looked into further, and it will be revisited in Section 4.3. Regardless of this amplitude problem, optimal desired times were found such that the end effector reached as far as it could (for that setting) without causing the solenoid valves to open several times, and tests were run anyway with close-to-closed needle valves.

3. Timescale Testing of RoboClam and Results

53 total tests were run in which the RoboClam end effector dug into a 33-gallon tank of soda lime glass beads using only in and out motions. These tests were run with the in/out needle valves ranging from fully opened to almost fully closed (such that the air flow speeds, and thus the in/out times, varied greatly), and they used the optimal in/out time settings determined in Section 2.3. The energetic “cost” of each test was calculated, as described in Section 1.3, and was then related to the measured end effector expansion and contraction times.

3.1 Running Timescale Tests

Each test was run by resting the end effector on top of the 33-gallon tank of soda lime beads, turning the needle valves to a predetermined pair of settings (as chosen in Section 2.1), setting the desired in/out times to the corresponding optimal in/out times (as determined in Section 2.3), and allowing RoboClam to dig until it reached an arbitrary stopping depth. The stopping depth was set at about 0.32m below the starting point of the tests, but the energy efficiency analysis was only conducted for the first 0.25m of digging. This cutoff for the analysis was chosen in order to avoid the “bottom effects” that the robot encounters as it nears the bottom of the tank. A visual representation of the robot’s vertical displacement over time, labeled with the stopping depth, bottom effects, and limits for analysis, is shown in Figure 3-1.

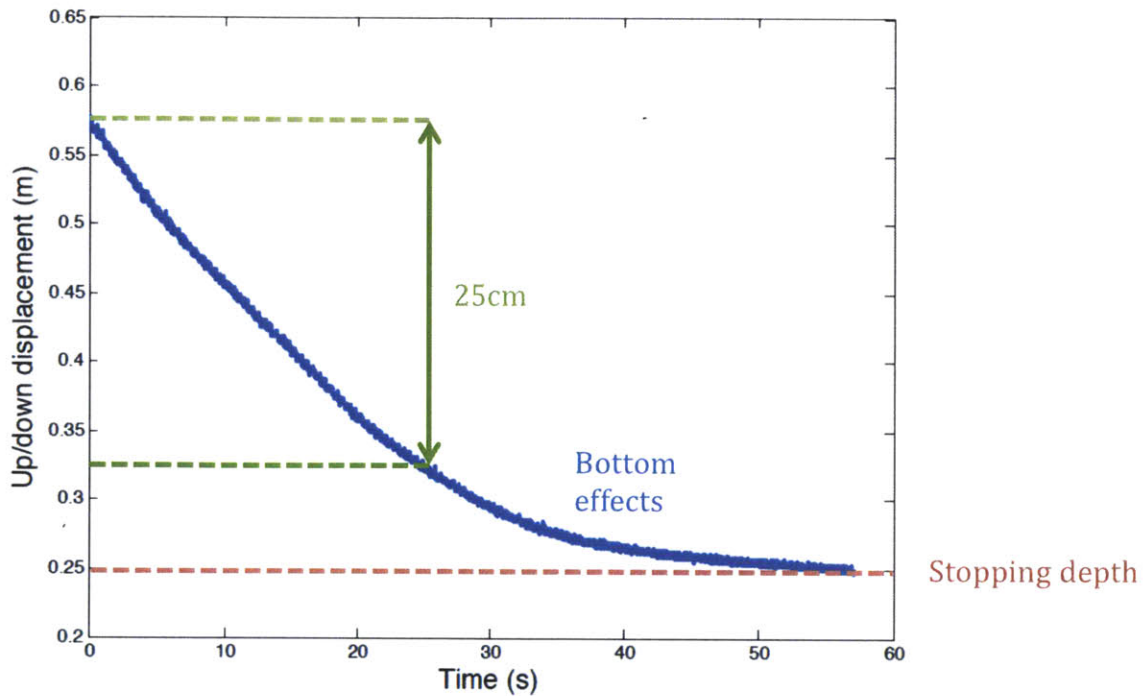


Figure 3-1: An example of the robot’s vertical displacement over time for a given trial. The stopping depth (labeled in red) is set arbitrarily at about 0.32m below the starting point, but the energy efficiency analysis is only done for the first 0.25m of digging, labeled in green. The analysis is cut off at this point to avoid the effects from the bottom of the container, labeled in light blue, which cause the robot to dig more slowly and less efficiently over time.

3.2 Results of Timescale Tests

After running each of these tests, the energetic “cost” analysis described in Section 1.3 was run on each test. The resulting power law relationship, α , was graphed in relation to the average measured expansion and contraction time for each test, just as was done on previous tests in Section 1.3. The results of this analysis are shown in Figure 3-2.

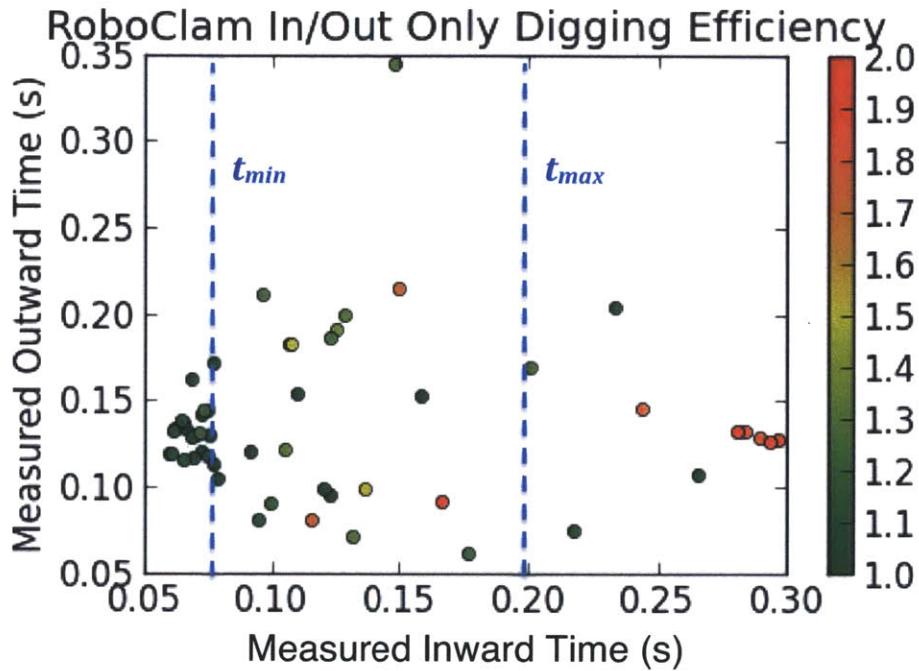


Figure 3-2: Results of 53 tests in varying the contraction and expansion times of RoboClam using needle valves. The color of the points correspond to the power law relationship α between energy and depth, where $E = \kappa\delta^\alpha$ and $\ln\kappa$ is the vertical intercept on the power law plot. Values of α close to 1 imply digging with localized fluidization, whereas values of α close to 2 imply digging in static soil. Timescales t_{min} and t_{max} correspond to the calculated minimum and maximum contraction times needed to achieve localized fluidization.

3.3 Observations from Test Results

The first thing to note from the results in Figure 3-2 is the fact that the cluster of green dots right around t_{min} , which first appeared in Figure 1-5, appears once again. This consistency between tests suggests that the new set of tests can be an adequate expansion on the old tests.

Another thing to note is that in the space between t_{min} and t_{max} , most dots are either green or light green (indicating that localized fluidization occurred), but there are

several yellow and red dots as well, indicating that this timescale area does not always lend itself to perfect fluidization.

Lastly, most points to the right of t_{max} are either red or orange, indicating that fluidization did not occur. This result is what was predicted by theory, as this is the area in which the particles should collapse and landslide around the end effector rather than fluidizing. Still, there are only a few tests that even fell into this category, so further testing will be needed to validate these findings.

As expected, the needle valves were not able to test the theoretical maximum expansion time (approximately 2.0s) because they were unable to slow down the end effector's expansion so drastically. However, the vertical spread in the tests did not indicate that there was any effect of the expansion time on whether or not fluidization occurred, so these results further validate the results of Figure 1-5.

4. Conclusions and Future Work

We conclude that the results found in this thesis support the theoretical timescale limits of RoboClam, but that further testing is needed to verify these conclusions. We suggest ways to automate and streamline the testing process, as well as guidelines for future work on RoboClam.

4.1 Conclusions

The results in Section 3.2 suggest that the area around t_{min} for contraction is optimal for low-energy burrowing, since that is the area where most of the green dots are concentrated in Figure 3-2. This makes sense because at approximately t_{min} , the soil particles will have enough time to catch up to the velocity of the contraction, but not have so much time that they begin to collapse or landslide into the void left by the contraction. As $t_{contract}$ gets larger, more particles start to collapse, and less soil fluidization is achieved. Therefore, the dots in Figure 3-2 slowly get yellower and redder as they move to the right. However, it does not seem that t_{max} is a hard cutoff for stagnant tests, seeing as there are a few tests where $t_{contract}$ is greater than t_{max} , but fluidization does occur. In order to determine with more certainty how energy efficiency changes with timescale, more tests will be needed (perhaps on the order of hundreds of tests). However, these tests could be run much more quickly and efficiently if they were automated.

4.2 Automating Tests

There are several potential benefits to automating these tests: they could be run more quickly, they would require far fewer labor hours, and they would be less susceptible to human error. Thus, automating tests should be the first priority in the continuation of this project. It would not be too difficult to automate the needle valves themselves; they could simply be connected to stepper motors. However, the larger challenge lies in automating the process of finding optimal desired in/out time settings. Since it was a trial and error process for the context of this thesis, a more theoretical approach will have to be used in the future. We will need to find the relationships between the settings of the needle valves (i.e. how many turns from open), the optimal desired in/out time settings (i.e. the settings found by trial and error before), and the actual measured in/out times (i.e. the axes on the graphs in Figure 1-5 and Figure 3-2). Once these relationships are established, in addition to the previously listed benefits, we will be able to run tests in essentially reverse order, by picking a point in the $t_{contract}$ vs. t_{expand} graph that we want to test, rather than by picking a pair of settings on the needle valves without knowing what part of the final graph they'll correspond to.

4.3 Varying Pressures with Flow Rates

The tests conducted for this thesis focused exclusively on varying the air flow rates to the pistons in order to change the expansion and contraction times of the end effector. However, in Section 2.3 we realized that when the needle valves got close to being closed, the amplitude of the expansion/contraction motions was diminished. We

speculated that this could be mitigated by increasing the pressures (as determined by the pressure regulators) as the air flow rates decreased. In order to confirm this theory, we'll need to find the relationships between the flow rates through the needle valves, the desired pressure settings, and the amplitude of the actual in/out motions of the robot. If we can find these relationships, we can use them to further standardize our tests by keeping the amplitude of the in/out motions constant in all tests.

5. Bibliography

[1] Winter, A., Deits, R., and Dorsch, D., 2013. "Critical timescales for burrowing in undersea substrates via localized fluidization, demonstrated by RoboClam: a robot inspired by Atlantic razor clams," Proc. ASME 2013 International Design Engineering Technical Conference, Portland, OR, pp. 1-6.

[2] Winter, A., 2011, "Biologically Inspired Mechanisms for Burrowing in Undersea Substrates," Ph.D. thesis, Massachusetts Institute of Technology, Cambridge, MA.

[3] Terzaghi, K., Peck, R., and Mesri, G., 1996. *Soil mechanics in engineering practice*. Wiley-Interscience.

[4] Robertson, P., and Campanella, R., 1983. "Interpretation of cone penetration tests. Part I: Sand". *Canadian Geotechnical Journal*, 20(4), pp. 718-733.

[5] Haupt, R., and Haupt, S., 2004. *Practical genetic algorithms*. Wiley-Interscience.